phys. stat. sol. (b) **149**, 45 (1988)

Subject classification: 61.70; 72.20; 78.60; S9.16

Raymond and Beverly Sackler Faculty of Exact Sciences, School of Physics and Astronomy, Tel Aviv University[1])

The Application of Thermally Stimulated Processes to the Study of Defects in Perovskite Type Fluorides

By

N. KRISTIANPOLLER, B. TRIEMAN, R. CHEN, and Y. KIRSH[2])

Thermally stimulated processes are studied in nominally pure, as well as in doped, perovskite type fluorides. The TSL and TSC, induced by X and monochromatic UV irradiations, are measured and their relations with other thermally stimulated processes are discussed. The excitation and emission spectra of the main TSL peaks are also measured, and their kinetic parameters are evaluated. From the comparison of the TSL and TSC curves, valuable information concerning the processes which occurred during the irradiation and the subsequent heating of the samples is obtained. The main TSL peaks seem to arise in this type of crystals from the thermal release of holes and their subsequent recombination with electron centres.

Thermisch angeregte Prozesse werden in reinen als auch in dotierten Fluoroperovskit-Kristallen untersucht. Die in diesen Kristallen durch Röntgen- oder durch monochromatische UV-Strahlung hervorgerufene TSL und TSC werden gemessen und deren Beziehungen zu anderen thermisch angeregten Prozessen werden erörtert. Die Anregungs- und Emissionspektren der TSL werden ebenfalls gemessen und die kinetischen Parameter werden berechnet. Aus dem Vergleich der TSL-Kurven mit denen der TSC werden wertvolle Informationen über die während der Bestrahlungen und während der darauf folgenden Ausheizung stattfindenden Vorgänge erhalten. Die wesentlichen TSL-peaks entstammen in diesen Kristallen anscheinend einer thermischen Befreiung von Defektelektronen und deren Rekombination mit Elektronzentren.

1. Introduction

Thermally stimulated luminescence (TSL) is known to be a very sensitive technique for the study of radiation effects in crystals. Additional valuable information can be obtained from the simultaneous measurement of TSL and electrical glow curves such as thermally stimulated conductivity (TSC) or exo-electron emission (TSEE). Some aspects concerning the simultaneous measurements of TSL, TSC, and TSEE are discussed in the next section. Experimental results obtained for various fluoroperovskite type crystals are reported and discussed in Sections 3 and 4. The simultaneous measurements of the TSL and TSC shed light on the defects produced by X and UV irradiations.

The crystals of the fluoroperovskite type can be described by the general formula ABF_3, where A is Li, Na, K etc., and B is Mg, Ba, Zn etc. Each A^+ ion is surrounded by twelve F^- ions, and each B^{2+} ion by six F^- ions. Some of these fluoroperovskite crystals, such as $KMgF_3$, are cubic, some are hexagonal (e.g. $RbMgF_3$) and others have an orthorhombic structure (e.g. $NaMgF_3$).

[1]) Tel Aviv 69978.

[2]) Permanent address: Everyman's University, 16 Klausner St., Tel Aviv 61392.

It has previously been found that fast electrons and γ-rays produce in these crystals defects, such as F, F^--aggregate, and V_k centres, similar to those produced in alkali halides [1 to 6]. It has also been shown that the same defects can be produced in some ABF_3 crystals by X-rays, and even by non-ionizing UV light, probably through a radiolysis process [7 to 9].

In the present work, the TSL and TSC induced by monochromatic UV irradiation in various fluoroperovskite crystals (nominally pure as well as doped) were recorded, and compared to the TSL and TSC induced in the same samples by X-irradiation. The kinetic parameters of the main TSL and TSC peaks were evaluated by the initial rise method and by Chen's half-width method [10]. In addition, the emission and excitation spectra of the TSL peaks were measured. In some of the samples, thermally stimulated polarization (TSP) and depolarization (TSD) currents were recorded as well.

2. Theory

The occurrence of TSL can be classified into two different categories. In one case trapped carriers (electrons or holes) are thermally raised to the conduction band (or the valence band, when holes are involved) prior to their recombination with carriers of the opposite sign, trapped in recombination centres. The other case is that of a local transition, in which the trapped carrier is thermally stimulated to an excited state within the forbidden gap and recombines with an opposite carrier in a close geometrical proximity [11]. The former case is characterized by the TSL peak being accompanied by TSC, whereas in the latter, no TSC peak occurs. Moreover, in the first case of carrier excitation into a fundamental band, the distinction between the release of electrons into the conduction band and holes into the valence band can be made by a TSEE measurement, in which the flow of electrons from the sample towards a positive electrode is recorded as function of the rising temperature. In cases where the mobile carriers are electrons, TSEE peaks will often accompany the TSC and TSL ones, whereas when the mobile carriers are holes, no such TSEE peaks are expected (for an unusual exception to this rule see [12]). In the present work we concentrate mainly on the case of thermal excitation of carriers into a fundamental band, namely in those instances where TSC peaks can be associated with TSL counterparts. For the simplicity of the discussion, let us assume that the mobile carriers are electrons, which are released from traps and subsequently recombine with trapped holes in recombination centres.

The rate equations governing the transitions between a single electron trapping state, the conduction band, and a single kind of hole recombination centre, are three simultaneous differential equations which cannot be analytically solved [11]. The best one can do is either to solve an approximate version of those equations or to solve them numerically for a given set of the relevant parameters. However, in order to study the relation between the TSL and TSC peaks, one can pursue a different route as follows. One of the three original differential equations is

$$-\frac{dm}{dt} = Amn_c\,, \tag{1}$$

where m (cm^{-3}) is the instantaneous concentration of holes in the centres, n_c (cm^{-3}) the instantaneous concentration of electrons in the conduction band, A ($cm^3\,s^{-1}$) the recombination probability, and t (s) the time [10, 11]. Both m and n_c are, of course, functions of time having initial values of m_0 and n_{c0}. Given a certain heating function $T = T(t)$ (e.g. a linear heating function $T = T_0 + \beta T$), $m(t)$ is always a decreasing

function of t whereas $n_c(t)$ is, in most cases, a peak shaped curve. The TSC peak is given by $n_c(t)$, while the TSL intensity $I(t)$ is assumed to be proportional to the recombination rate, and using appropriate units, this can be written as

$$I(t) = -\frac{dm}{dt}. \tag{2}$$

Assuming a given peak shaped function for $n_c(t)$, (1) is solved to give

$$m(t) = m_0 \exp\left[-A \int_0^t n_c(t')\, dt'\right], \tag{3}$$

and substituting into (1) and (2) yields

$$I(t) = A m_0 n_c(t) \exp\left[-A \int_0^t n_c(t')\, dt'\right]. \tag{4}$$

The condition for the maximum of the TSL peak is

$$\left(\frac{dn_c}{dt}\right)_{max} = A[n_c(t_{max})]^2, \tag{5}$$

where max indicates the time at which the TSL attains its maximum. Since the right hand side of (5) is positive, so is the left hand side and this indicates that the TSL peak reaches its maximum where $n_c(t)$ is still increasing. This proves that one should usually expect the TSL peak to precede the TSC one. These considerations do not indicate the amount of the shift between the two peaks. In certain cases the shift is so slight that the peaks seem to coincide, while in other cases a shift of several degrees has been recorded. An opposite shift has also been reported (though rarely) in the literature, which seems to be related to a temperature dependence of either the electron mobility, or the recombination probability A.

A method has also been developed [10] for the evaluation of A by the use of a simultaneous measurement of $n_c(t)$ and $I(t)$. Taking $I(t)$ at two points t_1 and t_2, one gets

$$\frac{I(t_2)}{I(t_1)} = \left[\frac{n_c(t_2)}{n_c(t_1)}\right] \exp\left[-A \int_{t_1}^{t_2} n_c(t)\, dt\right]. \tag{6}$$

All the quantities except for A can be measured, and thus A can be evaluated from (6).

This kind of analysis is apparently true, only if the TSL and TSC peaks originate from the same process. The occurrence of a local transition yielding TSL without TSC has already been mentioned. The opposite, namely, the recording of a TSC peak with no TSL counterpart can happen when non-radiative transitions are responsible for the deletion of free charge carriers.

If $n_c(T)$ is related to the release of electrons rather than holes, one can get additional information from TSEE measurements. The TSEE peak is given by the function $T^{1/2} \exp(-\varphi/kT)\, n_c(T)$, where φ is the work function required in order to release an electron into the vacuum. Since $n_c(T)$ is multiplied here by an increasing function of T, the TSEE peak is expected to occur at a higher temperature than its TSC counterpart. For the three phenomena, the expected order of appearence should therefore be TSL–TSC–TSEE.

If one tries to evaluate the activation energy by the very well known "initial rise" method, a value of $E + \varphi$ can be expected in TSEE. Other methods, such as the

"various heating rates" technique, should give the right value of E for the same TSEE peak [10]. Thus, the difference between the two values will give the work function φ.

In conclusion, if possible all three thermally stimulated processes are to be measured. The TSC results may sometimes be impaired by bad (non-ohmic) contacts. TSEE measurements seem to by-pass this difficulty. However, the fact that surface levels are often involved in exo-electron emission rather than bulk levels, may influence the conclusions one hopes to draw from simultaneous measurements.

3. Experimental Techniques

For our measurements, specimens of about 1 cm² cross section and 1 mm thickness were cleaved from the nominally pure or doped ABF_3 single crystals listed in Table 1. The samples were kept in a vacuum cryostat, equipped with three windows of fused silica for the UV irradiation and optical measurements, and an aluminium window, 0.3 mm thick, for X-irradiations. For irradiations in the vacuum UV (VUV) region, one of the fused silica windows was removed and the windowless cryostat was attached to a 1 meter normal incident UV monochromator (Mc Pherson 225) of a linear dispersion of 0.83 nm/mm. The slit width was normally 1 mm and a 1000 W hydrogen

Table 1

Temperatures (T), activation energies (E), and kinetic orders (b), of the main TSL and TSC peaks in X- and UV-irradiated ABF_3 crystals

crystal	TSL(X)			TSC(X)			TSL(UV)		
	T (K)	E (eV)	b	T (K)	E (eV)	b	T (K)	E (eV)	b
$LiBaF_3$	175	0.33	1.2	175	0.32	1	175	—	—
	218	0.58	1	240	—	—	215	—	—
	265	0.72	1.4				270	—	—
$KMgF_3:Ni^{2+}$	110	0.26	1.5	120	—	—			
	195	0.40	1.5	198	—	—	195	0.37	1.5
	290	0.51	2	292	0.47	1.2			
$KMgF_3:Eu^{2+}$	298	0.51	—	310	0.50	1	298	0.49	—
$NaMgF_3$	140	0.36	1.2	125	0.18	1			
				162	—	—			
				184	—	—			
	222	0.40	—	228	0.41	1			
	260	—	—	266	—	—			
	290	0.51	—				292	0.54	1.2
$RbMgF_3$	165	0.34	1	170	0.35	2	160	0.34	—
	206	0.38	2	198	0.38	2	198	0.39	2
	236	0.58	1.5	228	—	—	238	0.55	1
$RbMgF_3:Pb^{2+}$				168					
	183	0.37	1.5	188	0.36	1.5			
	327	0.85	1	328	0.87	1			
$KZnF_3$	148	0.24	1.6	162	0.23	1.5	152	0.23	1
				190	0.27	2			
	412	0.75	1	398	0.76	—	402	—	—

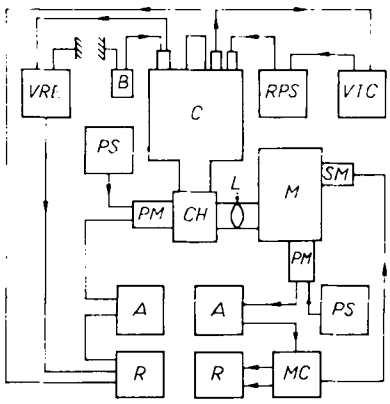

Fig. 1. Experimental set-up for simultaneous measurements of TSL and TSC glow curves and of TSL emission spectra. C and CH cryostat and holder attached to X-ray tube or monochromator, for X or UV excitation; PM, PS, A, and R photomultiplier, power supply, amplifier, and recorder; M grating monochromator for recording emission spectra; SM and MC stepping motor and control circuit; VTC thermocouple circuit, VRE and B electric circuit, consisting of batteries and a vibrating reed electrometer, for conductivity measurements. RPS controlled power supply

arc lamp was used as a light source. The incident photon flux was monitored by a sodium salicylate screen. The X-ray irradiations were carried out with a tungsten tube (45 kV, 15 mA). The VUV and X-irradiations were performed either at LNT or at RT. Optical absorption was measured before and after the irradiation, between 200 and 2000 nm, using a Cary-17 spectrophotometer. For absorption measurements in the VUV region, a double beam attachment was used with the McPherson monochromator [13].

TSL and TSC were measured simultaneously during heating of the irradiated samples at a constant rate of 10 K/min. The TSL was detected and amplified by an EMI 6256S photomultiplier and a microampermeter, and recorded on an x–y recorder.

For the electrical measurements, two gold coated electrodes were attached to one face of the crystal; the electric circuit consisted of a 500 V dc battery and a Cary 401 vibrating reed electrometer.

For measuring the emission spectra of the samples at the range 200 to 600 nm, a 0.5 m Bausch and Lomb grating monochromator was used. In order to enable the measurement of transient phenomena the monochromator was equipped with a fast scanning stepping motor, controlled by an electronic system. The slit width of the monochromator for detecting weak emission spectra was up to 1 mm. Spectra were normally scanned in both directions at a speed of 20 nm/s.

The experimental set-up which enabled us to measure simultaneously the electrical and optical glow curves as well as the emission spectra of the TSL emission, is shown in Fig. 1.

For measuring the TSD current, the sample was cooled to 80 K under an external field and then heated up with its electrodes short-circuited through the microampermeter. The TSP current was recorded while the sample was heated up from 80 K under an external field, after being cooled in the absence of the field.

4. Experimental Results

Both X and VUV irradiations at 80 K caused noteable TSL peaks in the various ABF_3 crystals, during the heating from 80 to 600 K. Most of the X-irradiated crystals exhibited TSC peaks as well, but no TSC could be detected in the VUV irradiated crystals. Prolonged X-irradiations at 80 K caused the appearance of various absorption bands characteristic of the specific crystal. No such bands could be detected after VUV irradiations of the examined crystals.

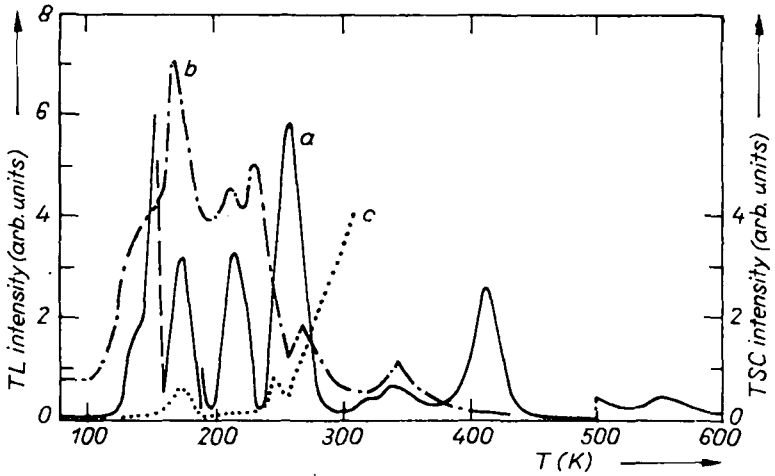

Fig. 2. TSL and TSC glow curves of $LiBaF_3$. (a) TSL after X-irradiation at 80 K (the 175 K peak is reduced by a factor of 10 and the 552 K peak is enlarged by a factor of 300), (b) TSL after VUV irradiation (160 nm), (c) TSC after X-irradiation at 80 K

In Fig. 2, an example of TSL and TSC glow curves is shown, for $LiBaF_3$. Curve a is the TSL recorded after X-irradiation at 80 K, and curve b the TSL of the same sample after monochromatic VUV irradiation at 160 nm. Curve c shows the X-induced TSC. It can be seen that except for differences of relative intensities, essentially the same TSL peaks appear after X and UV irradiation. Two main peaks in the X-induced TSL curve are accompanied by current peaks. The rise of the ionic conductivity prevents the study of the TSC curve above 300 K. In Fig. 3 and 4, similar results are shown for Ni and for Eu doped $KMgF_3$ crystals. In $KMgF_3:Ni^{2+}$ all the four X-induced TSL peaks are accompanied by TSC peaks, while in $KMgF_3:Eu^{2+}$ there is one prominent peak at 298 K and its TSC counterpart appears at 310 K. In

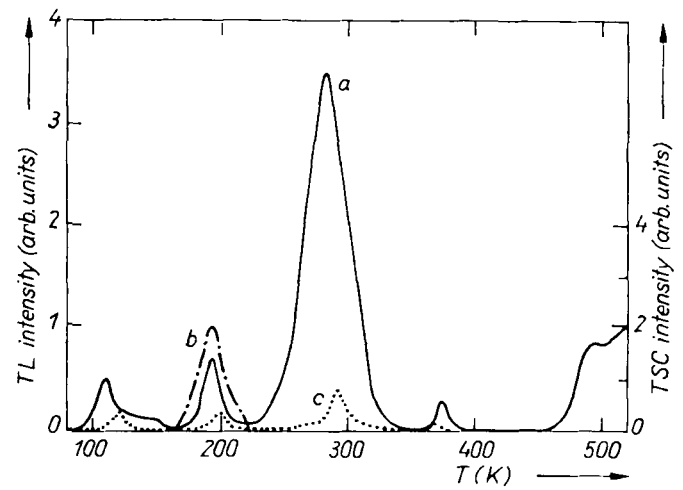

Fig. 3. TSL and TSC glow curves of $KMgF_3:Ni^{2+}$ following X- or UV-irradiation at 80 K. (a) X-induced TSL (reduced by 10^4), (b) TSL induced by 140 nm irradiation, (c) TSC induced by X-irradiation

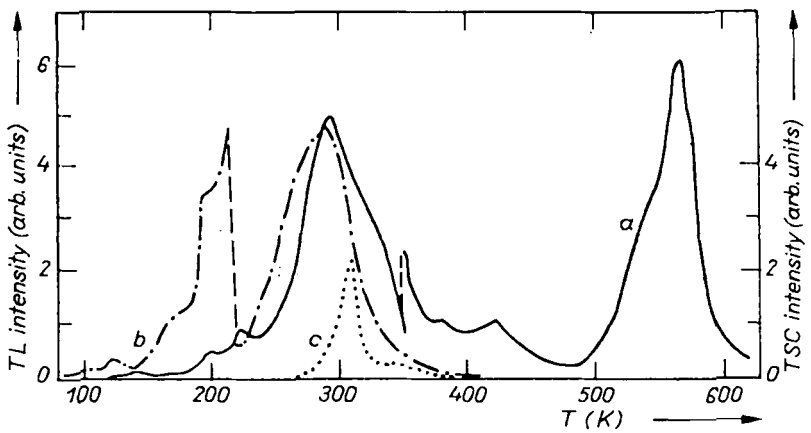

Fig. 4. TSL and TSC glow curves of $KMgF_3:Eu^{2+}$. (a) TSL induced by X-irradiation at 80 K (the curve up to ≈360 K is reduced by a factor of 3), (b) TSL induced by 160 nm at 80 K (the curve up to ≈220 K is enlarged by a factor of 10), (c) TSC induced by X-irradiation at 80 K

other ABF_3 crystals we also found that the main TSL peaks after X irradiation were accompanied by TSC peaks. The temperatures of the main TSL and TSC peaks, together with their average activation energies and order of the reactions, are summarized in Table 1.

In Fig. 5 examples of the TSL emission spectra are given for X-irradiated nominally pure $KMgF_3$. Curves a, b, c, d were recorded at the temperatures: 145, 198, 378, and 540 K, respectively. Clear emission bands appear at 225, 320, and 460 nm.

The excitation spectra of the UV-induced TSL in the various crystals showed maxima typical of the specific crystal. In Fig. 6, excitation spectra are shown for nominally pure $NaMgF_3$.

Weak current peaks which were recorded in most of the crystals even without any prior irradiation, appear to be TSP currents, due to the motion of dipoles. The TSP

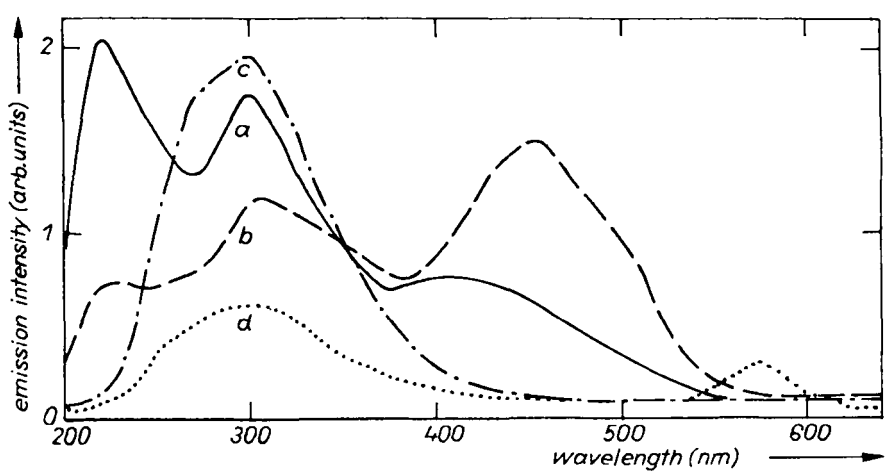

Fig. 5. TSL emission spectra of X-irradiated $KMgF_3$, recorded at the following peaks: (a) T — 145 K (the curve is enhanced by a factor of 3), (b) 198, (c) 378, (d) 540 K (the curve is enhanced by a factor of 100)

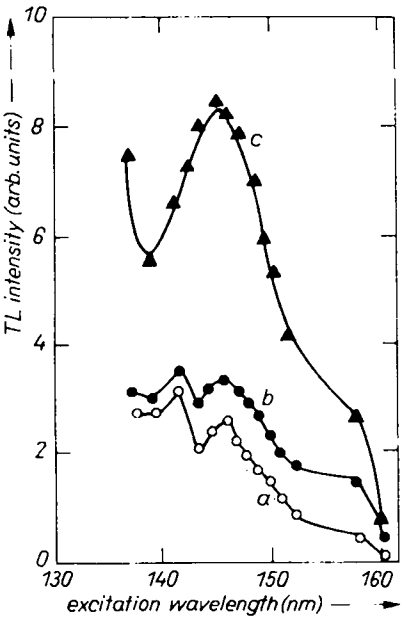

Fig. 6

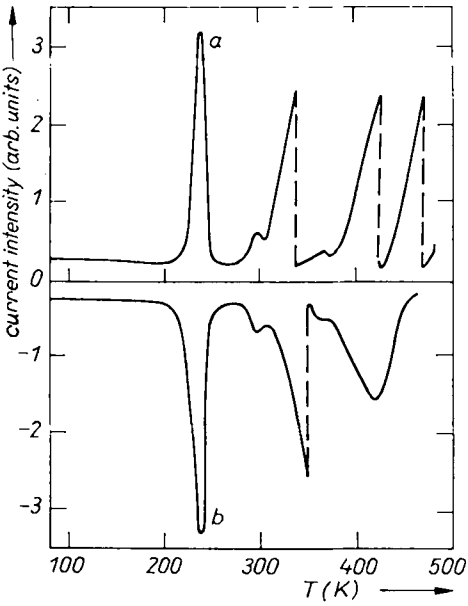

Fig. 7

Fig. 6. Excitation spectra of the main TSL peaks in $NaMgF_3$ irradiated by VUV light at 80 K. The peaks are at (a) T = 292, (b) 365, and (c) 450 K

Fig. 7. (a) Thermally stimulated polarization current (PTC) and (b) thermally stimulated depolarition current (ITC) in $KZnF_3$

curve of $KZnF_3$ is shown in Fig. 7, curve a. Curve b is the TSD (or ionic thermocurrent, ITC) curve of the same sample. It is known that TSD peaks which involve the motion of dipoles, have "mirror peaks" in the TSP curve ([10] p. 76). Thus, the comparison between the two curves indicates that the TSD peaks at about 235, 300, and 370 K are due to the re-orientation of dipoles, while the 420 K peak involves the transport of charge carriers.

5. Discussion

A correlation was found between TSL peaks in X-irradiated ABF_3 crystals and the thermal decay of certain absorption bands induced by the irradiation [7 to 9]. From this correlation, and from the emission spectra of the TSL peaks [7, 8], it was deduced that the main hole centres produced by the irradiation at 80 K are V_k, or self-trapped hole centres, in which the hole is trapped between two F^- ions. The most common electron centre was found to be the F-centre (an electron trapped at a vacancy of F^-). The electron centres are thermally stable up to relatively high temperatures. However, the V_k centres become mobile at various temperatures between 110 K and RT, and recombine with electron centres. The fact that most of the main TSL peaks are accompanied by TSC, indicates that these recombinations are not local transitions, but involve charge transport over several unit cells.

In $LiBaF_3$, for example (Fig. 2), all the TSL peaks were ascribed to the recombination of holes, released from V_k centres, with F-centres [9]. The TSC peaks are quite weak, but it can be seen that they accompany the main TSL peaks. This is seen even

more clearly in $KMgF_3:Ni^{2+}$ (Fig. 3). The 110 K peak was attributed to the motion of self-trapped holes along the columns of F^- ions in the ⟨110⟩ direction [14]. The peaks at $\approx$ 300 K in the Ni^{2+} and Eu^{2+} doped crystals, were ascribed to V_k stabilized by Na^+, which substitutes for a lattice K^+ ion [14]. In $KMgF_3:Eu^{2+}$ the TSL peaks at 145, 198, and 225 K, which have activation energies of 0.35 to 0.42 eV, are not accompanied by TSC. They are probably due to the motion of neutral fluorine interstitial atoms (F_0) which recombine with F-centres to yield self-trapped excitons (STE). We found that the emission spectra of these peaks contain a band at 310 nm which had been ascribed to the luminescence of STE in fluorides [15]. A similar band appears in the TSL emission spectra of nominally pure $KMgF_3$ (Fig. 5).

In $NaMgF_3$, a strong TSL peak appears at 100 to 160 K, with its maximum at 140 K (see Table 1). Only the low temperature part of this peak is accompanied by TSC (peaked at 125 K). The TSL emission spectra indicated that two recombination processes occur in this temperature range [7]. It has previously been suggested that in the first part of this TSL peak, in electron irradiated samples, the main process is a recombination of the first of two intrinsic V_k centres typical for this crystal, with F-centres [16]. The dominant process in the second part was ascribed to recombinations of F^0 interstitials with F-centres [16]. Our present results, in X- as well as in UV-irradiated crystals, are in accordance with this suggestion. From Table 1 one can see that the first process, the activation energy of which is $\approx$ 0.2 eV, causes a TSC peak as well, while the second process is not associated with TSC, due to the neutrality of the F^0 interstitials. The activation energy for the F^0 motion is $\approx$ 0.36 eV. The TSC peaks at 162 and 184 K, which appear to have no TSL counterparts, are probably due to the motion of charge carriers, such as F^- interstitials, which does not result in radiative recombinations. The 168 K TSC peak in $RbMgF_3:Pb^{2+}$ and the 190 K one in $KZnF_3$ might be due to similar processes.

The 222, 260, and 290 K TSL peaks in $NaMgF_3$ showed similar emission spectra which had been previously ascribed to the recombination of holes with F-centres [16]. In the present work we found that the first two are accompanied by TSC peaks. The 290 K TSL peak, which coincides with the decay of the second intrinsic V_k centre [16], is not accompanied by TSC, and may involve a local transition between the V_k and a nearby F-centre, rather than a motion through the valence band.

The three main TSL peaks of $RbMgF_3$ were ascribed to the recombination of holes from extrinsic V_k centres, with electron centres [4]. The emission spectra of the 206 and 236 K peaks are essentially the same, while the 165 K peak presents a different emission spectrum [8] indicating that the recombination processes might be different. In the present work we have found another difference between the first peak and the two other ones. Contrary to most of the peaks in Table 1, and to the theory presented in Section 2, the TSC peaks at 198 and 228 K precede their TSL counterparts (at 206 and 236 K). This might be an indication that the process here is more complicated than a simple hole–electron recombination.

In $RbMgF_3:Pb^{2+}$ the Pb^{2+} ions act to stabilize the hole centres [8]. This is supported by the fact that the first main TSL–TSC peak in our work occurs at a higher temperature, and with a higher activation energy, than in the nominally pure crystal. In $KZnF_3$, the 148 K TSL peak was ascribed to an extrinsic V_k, stabilized by a cationic vacancy, probably of Zn^{2+} [2]. The origin of the 412 K TSL peak is not yet clear.

Our experimental results showed that in most of the examined crystals TSL could be excited not only by X-rays, but by monochromatic UV radiation as well. The UV-induced TSL peaks were generally weaker than the X-induced peaks, but appeared at approximately the same temperatures, and with the same activation energies (see Table 1). This indicates that the glow peaks are due in both cases to the same defects.

It should be noted, however, that some of the prominent peaks in the X-induced glow curves did not appear after UV irradiations (see for example Fig. 3). These peaks are probably associated with defects which can not be created by the lower energy UV photons.

We have also found that the main TSL peaks in the X-irradiated samples were accompanied by TSC, while the UV irradiation failed to stimulate any detectable TSC in the crystals. This might be partially due to the smaller concentration of defects formed by the UV light. In some cases, however, the intensity of the UV-induced TSL was comparable to that of the X-induced TSL, and yet, TSC peaks appeared only in the X-irradiated samples. A plausible explanation might be, that the UV light causes the formation of hole and electron centres in close proximity, so that the recombination is either through a local transition, or a process in which the charge carriers are in the band for a very short time. More research is required in order to investigate this assumption.

The TSD and TSP currents (Fig. 7) show that the unirradiated crystals contain dipoles, probably impurity ions in the vicinity of their charge compensators. The study of the influence of the UV- and X-irradiations on these dipoles might improve our knowledge concerning the irradiation effects in these crystals.

References

[1] C. R. RILEY and W. A. SIBLEY, Phys. Rev. B **1**, 2789 (1970).
[2] L. A. KAPPERS and L. E. HALLIBURTON, J. Phys. C **7**, 589 (1974).
[3] R. ALCALA, N. KOUMVAKALIS, and W. A. SIBLEY, phys. stat. sol. (a) **30**, 449 (1975).
[4] N. KOUMVAKALIS and W. A. SIBLEY, Phys. Rev. B **13**, 4509 (1976).
[5] W. A. SIBLEY and N. KOUMVAKALIS, Phys. Rev. B **14**, 35 (1976).
[6] J. R. SERETLO, J. J. MARTIN, and E. SONDER, Phys. Rev. B **14**, 5404 (1976).
[7] N. KRISTIANPOLLER and B. TRIEMAN, J. Physique, **41**, C6–109 (1980).
[8] B. TRIEMAN and N. KRISTIANPOLLER, phys. stat. sol. (b) **105**, 739 (1981).
[9] N. KRISTIANPOLLER and B. TRIEMAN, Radiat. Eff. **72**, 201 (1983).
[10] R. CHEN and Y. KIRSH, Analysis of Thermally Stimulated Processes, Ch. 2 and 6, Pergamon Press, 1981.
[11] A. HALPERIN and A. A. BRANER, Phys. Rev. **117**, 408 (1960).
[12] G. HOLZAPFEL, Proc. VI Internat. Symp. Tech. Comm. Photon Detect., Siofok (Hungary), 1974 (p. 30).
[13] M. SCHLESINGER and T. SZCZUREK, Rev. sci. Instrum. **44**, 1729 (1973).
[14] J. E. RHOADS, B. H. ROSE, and L. E. HALLIBURTON, J. Phys. Chem. Solids **37**, 346 (1975).
[15] W. HAYES, Crystals with the Fluorite Structure, Clarendon Press, Oxford 1974 (p. 237).
[16] M. A. YOUNG, E. E. KOHNKE, and L. E. HALLIBURTON, Bull. Amer. Phys. Soc. **21**, 439 (1976).

(Received April 27, 1988)